

18 **Abstract**

19 The mechanisms underlying the functional differences in sympathetic and parasympathetic regulation of
20 the major salivary glands have received little attention. The acute effects of parasympathetic muscarinic
21 (carbachol)-dependent and combined parasympathetic-dependent + cAMP-dependent pathways on fluid
22 secretion rates, ion composition and protein content were assessed using a newly developed *ex vivo*
23 preparation that allows the simultaneous perfusion of the mouse submandibular (SMG) and sublingual
24 (SLG) glands. Our results confirm that the muscarinic dependent pathway accounts for the bulk of
25 salivation in SMG and SLG while co-stimulation with a cAMP-increasing agent (forskolin, isoproterenol,
26 or vasoactive intestinal peptide) did not increase the flow rate. Co-stimulation with carbachol + the β -
27 adrenergic agonist isoproterenol decreased the concentration of NaCl and produced a substantial increase
28 in the protein and Ca^{2+} content of SMG but not SLG saliva, consistent with a sparse sympathetic
29 innervation of the SLG. On the other hand, Forskolin, which bypasses receptors to increase intracellular
30 cAMP by directly activating the enzyme adenylate cyclase, enhanced the secretion of protein and Ca^{2+} by
31 both the SMG and SLG. In contrast, isoproterenol and vasoactive intestinal peptide specifically
32 stimulated protein secretion in SMG and SLG salivas, respectively. In summary, cAMP-dependent
33 signaling does not play a major role in the stimulation of fluid secretion in SMG and SLG while each
34 cAMP-increasing agonist behaves differently in a gland-specific manner suggesting differential
35 expression of G-protein coupled receptors in the epithelial cells of SMG and SLG.

36

37 **Introduction**

38 Saliva is a complex fluid mainly composed of secretions from the major glands and hundreds of minor
39 salivary glands that drain into the oral cavity where it plays many important roles such as lubrication of
40 oral mucosal surfaces, demineralization and remineralization of teeth, food digestion and control of the
41 oral microbiome (26). The importance of saliva is clearly inferred from patients suffering from diseases
42 that are associated with salivary gland hypofunction such as Sjögren’s syndrome or as the consequence of
43 radiotherapy in head and neck cancers (22).

44 In humans, the major salivary glands (parotid, submandibular and sublingual glands) secrete between 0.5-
45 1 liter of saliva per day. This efficiency is achieved because acinar secretory cells express ion-transporting
46 proteins in their apical and basolateral domains that allow vectorial secretion of solutes and fluid into the
47 luminal space (25).

48 Salivary gland function is regulated by the parasympathetic and sympathetic branches of the autonomic
49 nervous system. It is known that sympathetic, adrenergic stimulation of parotid and submandibular glands
50 results in the secretion of low amounts of a protein-rich fluid with a very low NaCl content. Conversely,
51 parasympathetic, cholinergic stimulation of parotid and submandibular glands is associated with copious
52 amounts of fluid containing comparatively low amounts of proteins and a relatively higher NaCl
53 concentration (3, 28).

54 Although the molecular mechanism underlying fluid secretion is well conserved among salivary glands
55 (15), the regulation of ion transport and fluid secretion processes apparently differ between glands. It is
56 known that parotid and submandibular glands receive inputs from sympathetic and parasympathetic
57 fibers, where they modulate ion transport as well as fluid and protein secretion (22, 27). In contrast,
58 mucous-secreting minor and sublingual glands receive extensive inputs from the parasympathetic system
59 but the innervation by the sympathetic system is sparse (26).

60 Protein secretion by the rat sublingual gland is modulated by the parasympathetic activation of
61 cholinergic muscarinic receptors in a PKC-dependent manner (8). The role of the sympathetic system on
62 protein secretion by the sublingual gland is contradictory. It has been reported that sympathetic adrenergic
63 agonists do not stimulate mucin secretion by isolated rat sublingual gland cells (7), while the amount and
64 concentration of protein in the saliva from rat sublingual glands increased upon intraperitoneal injection
65 of catecholamines compared to cholinergic agonists (1).

66 On the other hand, little is known about the modulation of protein and fluid secretion of mucous-secreting
67 glands by cAMP-dependent pathways. Vasoactive intestinal peptide (VIP) is a parasympathetic-
68 associated neurotransmitter that raises intracellular cAMP levels and have been reported to modulate the
69 exocytosis of protein-storing granules in human major salivary gland acinar cells (9). Furthermore,
70 intravenous injections of VIP induced saliva secretion by the rat parotid and submandibular glands (11).
71 Of note, increased levels of VIP are observed in the parotid and submandibular glands of
72 sympathectomized rats, suggesting a compensatory mechanism mediated by these cAMP-raising
73 secretagogues in the absence of β -adrenergic receptor-mediated, cAMP cell signaling (10). Nonetheless,
74 the negligible sympathetic innervation of mucous-secreting glands raises the question of which, if any,
75 physiological secretagogues that increase intracellular cAMP levels might be involved in the regulation of
76 fluid and protein secretion in the mucus-secreting sublingual salivary glands.

77 Taken together, we hypothesize that cAMP-dependent pathways might regulate the activity of mucus-
78 secreting salivary glands. To test this model, we developed an *ex vivo* assay for simultaneously assessing
79 the role of cAMP-raising secretagogues in mouse serous-secreting submandibular (SMG) and mucous-
80 secreting sublingual (SLG) glands. Our results show that cAMP-dependent mechanisms differentially
81 regulate serous- and mucous-secreting glands.

82

83

84 **Materials and Methods**

85 ***Ex vivo perfused SLG and SMG***

86 *Ex vivo* SLG and SMG salivas were simultaneously collected by modifying the *ex vivo* mouse SMG
87 perfusion technique (30). In brief, mice were anesthetized by chloral hydrate injection (400 mg/kg i.p.)
88 and all branches of the common carotid artery were ligated, except for the artery supplying blood to SLG
89 and SMG. Both glands were then removed and perfused at 37°C via the common artery, which was
90 cannulated with a 31G cannula. SLG and SMG ducts were placed in different calibrated glass capillary
91 tubes (Figure 1). Salivation was stimulated by perfusion with the muscarinic receptor agonist carbachol
92 (CCh, 0.3 µM) or CCh (0.3 µM) + cAMP-increasing agents (5 µM isoproterenol, 100 nM vasoactive
93 intestinal peptide or 10 µM forskolin). The perfusion solution was (mM): 4.3 KCl, 120 NaCl, 25
94 NaHCO₃, 1 CaCl₂, 1 MgCl₂, 5 glucose, and 10 Hepes, pH 7.4 (gassed with 95% O₂/5% CO₂). Saliva
95 samples were collected and stored at -80°C until analyzed.

96 ***Ion and protein concentrations in SLG- and SMG-secreted fluids***

97 Na⁺, K⁺ and Ca²⁺ concentrations in saliva were measured by atomic absorption spectrometry using the
98 appropriate lamps (AAAnalyst 200 spectrometer, PerkinElmer). The Cl⁻ concentration was analyzed with
99 an Orion™ Cl⁻ electrode (Thermo Fisher Scientific). To insure enough sample for measuring the ion
100 composition of saliva secreted in response to cAMP-raising secretagogues, data shown in Figures 3 and 4
101 were obtained from SMG and SLG stimulated for 15 minutes.

102 Protein concentrations were measured according to the manufacturer's instructions by the micro-BCA
103 assay (Thermo Fisher Pierce, Rockford, IL, USA) using a DU530 spectrophotometer (Beckman) at 562
104 nm. Bovine serum albumin was used as standard for calibrations. Protein concentrations were calculated
105 from SMG and SLG stimulated for 5 minutes with agonist. This time window was chosen for the protein
106 measurements shown in Figures 5 and 6 as 75% of amylase (one of the most abundant protein in saliva) is
107 secreted within the first 5 minutes in response to stimulation in rat parotid slices (14).

108 ***Gene expression analysis***

109 Gene expression analysis of β -adrenergic and VIP receptors and the $K_{Ca1.1}$ (*Kcnma1*) K^+ channel was
110 performed using publicly available RNA-sequencing data of mouse major salivary glands (SRA databases
111 SRX2648311 to SRX2648322; n=12) (13). Threshold for positive gene expression was 0.1 FPKM
112 (fragments per kilobase of transcript per million of mapped reads). Gene-sequencing data from salivary
113 glands from 3 females and 3 male mice were used for comparing gene expression levels between
114 submandibular and sublingual glands.

- 115 1) The *Kcnma1* mRNA expression levels for SMG and SLG from RNA-Seq data reported as FPKM
116 values were 4.47 ± 0.55 vs. 1.21 ± 0.08 (average \pm SEM; SMG vs. SLG, respectively; n=6 each
117 gland, p value < 0.005 , Student's t test).
- 118 2) The β -adrenergic receptor expression levels (FPKM) were 5.15 ± 1.16 vs. 0.41 ± 0.12 for *Adrb1*
119 and 3.61 ± 0.50 vs. 1.30 ± 0.41 for *Adrb2*, SMG vs. SLG, respectively (n=6 each gland, p value $<$
120 0.005 , Student's t test).
- 121 3) VIP receptor mRNA levels (FPKM) of type 1 VIP receptor (*Vipr1*) for SMG vs. SLG were $0.49 \pm$
122 0.06 vs. 3.31 ± 0.18 ; n=6 each gland, p value < 0.005 , Student's t test. Transcript levels for type 2
123 VIP receptors encoded by *Vipr2* were very low in both SMG and SLG (FPKM values < 0.1).

124 ***Statistical Analysis***

125 Results are presented as the mean \pm standard deviation (SD). Individual data points are shown in box
126 graphs. Statistical significance was determined using Student's t test and one-way ANOVA analysis
127 followed by Bonferroni's *post hoc* test. P values of less than 0.05 were considered statistically significant.
128 Origin 8.0 Software was used for statistical calculations (OriginLab, Northampton, MA, USA).

129

130

131 ***Animals and Reagents***

132 Mice (BS/129Svj background) were housed in cages with access to laboratory chow and water *ad libitum*
133 with a 12-hour light/dark cycle. BS/129Svj background mice was generated in house by crossing BS
134 (Charles River Laboratories) and 129Svj (The Jackson Laboratory) mice. Equal numbers of sex- and age-
135 matched (from 6 to 12 wk old) mice were utilized. All animal procedures were approved by the Animal
136 Care and Use Committee of the National Institute of Dental and Craniofacial Research, National Institutes
137 of Health (ASP 13-686). All reagents were from Sigma-Aldrich (St.Louis, MO, USA), unless otherwise
138 indicated.

139 **Results**

140 ***Saliva secretion by simultaneous ex vivo perfusion of SMG and SLG***

141 Saliva formation is a two-step process where a NaCl-rich, plasma-like fluid is secreted by acinar cells
142 (stage 1). The ion composition of this primary fluid is subsequently modified (mainly NaCl reabsorption
143 and KHCO₃ secretion) as it passes through the ductal epithelium (stage 2) (22, 25). Given that ductal
144 function in salivary glands is regulated by β-adrenergic receptors (5), we evaluated the effect of
145 muscarinic (CCh) plus β-adrenergic (Isoproterenol, IPR) receptor stimulation on SMG and SLG flow
146 rates and ion composition. As seen in Figure 2, a slight but significant reduction in flow rates was
147 observed in SMG (Figures 2A-B) and SLG (Figures 2E-F) secretion rates when the β-adrenergic agonist
148 IPR (5 μM) was co-perfused with the muscarinic agonist CCh (0.3 μM). In terms of duct function, IPR
149 and CCh co-stimulation induced a substantial NaCl reabsorption in SMG (Figure 2C; 38% decrease in
150 [Na⁺] + [Cl⁻]) but not in SLG-secreted fluid (Figure 2G). Moreover, the K⁺ concentration of SMG saliva
151 did not differ between CCh- and CCh/IPR-stimulated glands (Figure 2C) while the K⁺ content of SLG
152 saliva was slightly reduced upon β-adrenergic receptor stimulation with IPR (Figure 2G). Of note, the
153 Ca²⁺ concentration of SMG saliva increased ~140% but did not significantly change in SLG upon β-
154 adrenergic receptor activation by isoproterenol (Figures 2D and 2H, respectively).

155 We then evaluated the effects of other physiological secretagogues that raise intracellular cAMP levels on
156 SMG and SLG function. To assess if cAMP secretagogues affect the secretory (acinar) function of SMG
157 (Figures 3A-B) or SLG (Figures 3C-D), the flow rates were measured in response to 0.3 μ M CCh or
158 combined stimulation with CCh (0.3 μ M) plus forskolin or VIP. As seen in Figures 3A-B and 3C-D,
159 comparison of SMG and SLG secretion rates during 15-minute stimulation showed that forskolin, which
160 directly activates adenylate cyclase, reduced CCh-mediated flow rates in both SMG and SLG,
161 respectively.

162 To evaluate if ductal function in SMG and SLG are modulated by cAMP-raising secretagogues, we then
163 evaluated the ion composition of the SMG- and SLG-secreted fluids collected in response to the
164 experimental conditions shown in Figure 3. As seen in Figure 4, the Na⁺, K⁺ and Cl⁻ compositions of
165 SMG- and SLG-secreted salivas were differentially affected by different cAMP secretagogues: *i.* NaCl
166 content in saliva from SMGs stimulated with by forskolin or VIP were statistically equal to NaCl content
167 from SMG-secreted saliva in response to CCh (Figures 4A-B); *ii.* K⁺ content in saliva collected from
168 SMG co-stimulated with CCh and forskolin was statistically less from all the other groups tested (Figure
169 4C); *iii.* Reduction in Na⁺ (Figure 4E) and K⁺ (Figure 4G) content in SLG saliva co-stimulated with VIP
170 was statistically different from SLG fluids stimulated with CCh or co-stimulation with forskolin; *iv.* K⁺
171 content in saliva from SLG glands stimulated with CCh + forskolin secreted a fluid with lower K⁺
172 content; and, *v.* none of the cAMP-inducing agonists tested in this study modified the Cl⁻ content
173 compared to its control (0.3 μ M CCh; Figures 4A and 4F). Regarding the Ca²⁺ content of saliva, co-
174 stimulation with CCh + forskolin resulted in higher [Ca²⁺] in the salivas of both SMG and SLG. In
175 contrast, VIP did not induce a significant increase in Ca²⁺ content in SMG or SLG saliva (Figures 4D and
176 4H, respectively).

177 ***Protein secretion in saliva from perfused SMG and SLG***

178 It has been shown that a higher protein concentration in saliva is associated with sympathetic activity in
179 parotid and SMG glands. Given that the SLG gland receives a sparse innervation of sympathetic fibers,

180 little is known about the regulation of protein secretion in SLG by agonists that raise intracellular cAMP
181 levels (7, 26, 27). Taking advantage of the simultaneous SMG and SLG perfusion technique described
182 here, we measured the protein concentration in SMG and SLG salivas obtained by perfusion of both
183 glands with solutions containing different agonists.

184 We first compared protein concentrations and calculated the total amount of protein secreted from both
185 SMG and SLG stimulated for 5 minutes with CCh and CCh + IPR, respectively. Figures 5A-C show that
186 the protein concentration and the amount of protein secreted by the SMG gland was substantially
187 stimulated nearly 3-fold upon β -adrenergic receptor stimulation. In contrast, no difference was observed
188 in the protein concentration and the amount of protein secreted from SLG glands stimulated with CCh
189 compared to CCh+ IPR (Figure 5D-F).

190 We then evaluated the protein concentration and amount of protein secreted by SMG and SLG co-
191 stimulated with CCh and different cAMP-raising secretagogues. Figures 6A-C show that forskolin and
192 VIP increased the amount and concentration of protein secreted compared to SMG stimulated with CCh.
193 Similarly, the amount and concentration of protein in SLG saliva increased when SLG glands were co-
194 stimulated with CCh and forskolin or VIP (Figure 6D-F).

195 **Discussion**

196 The molecular mechanism underlying fluid secretion in mammalian salivary glands is well conserved (20,
197 22, 25). Briefly, the basolateral domain of secretory acinar cells express Na⁺/K⁺ ATPase (21), Na⁺-K⁺-2
198 Cl⁻ cotransporter (12, 21) and K⁺ channels (3, 24, 28, 30), which promote the intracellular accumulation
199 of Cl⁻ above its equilibrium potential. Apical Ca²⁺-activated Cl⁻ channels allow Cl⁻ efflux across the
200 luminal membrane, which creates a negative transepithelial potential difference that drives Na⁺ secretion
201 into the luminal space via the paracellular pathway (4, 29, 32). Finally, NaCl accumulation generates an
202 osmotic gradient that energizes the water movement in the secretory direction via transcellular (aquaporin
203 5-dependent) and paracellular pathways (16, 19). Key proteins involved in fluid secretion have been
204 found in acinar cells from all major salivary glands (15). However, the major salivary glands display
205 distinct secretory properties, i.e. the contribution of each gland to whole saliva differs in terms of ion and
206 protein content and the stimuli that trigger secretion.

207 In this study, we evaluated the dependence of acinar cell fluid secretion on β-adrenergic receptor
208 stimulation in SMG and SLG. As seen in Figure 2, co-stimulation with CCh + isoproterenol slightly
209 decreased the flow rates of both SMG and SLG (<15%). In contrast, the physiological cAMP-raising
210 agonist VIP had no effect on the flow rates displayed by SMG and SLG in response to muscarinic
211 receptor stimulation. Our results contrast with those reported by Larsson et al. where CCh-induced *in vivo*
212 salivation by rat parotid gland is potentiated by forskolin and VIP (18). We do not have a clear
213 explanation for such differences but the *in vivo* pro-stimulatory effect of forskolin and VIP might be due
214 to systemic effects that are not present in the isolated perfused-gland preparation.

215 Sympathetic fibers innervate the ducts of the parotid and SMG, where stimulation enhances NaCl
216 reabsorption, while the sympathetic innervation in SLG is sparse (26). Consistent with these anatomical
217 observations, reabsorption of NaCl was strongly activated upon β-adrenergic receptor stimulation in SMG
218 but not in SLG. On the other hand, the NaCl content of SMG saliva produced by CCh co-stimulation with

219 VIP did not differ from stimulation with only CCh (Figure 4A-B). This finding suggests that VIP
220 receptors are not expressed at significant levels in the SMG duct cells responsible for NaCl reabsorption.
221 Alternatively, we cannot rule out that VIP-mediated signals can inhibit ductal function in SMG ducts.
222 Co-stimulation of SLGs with CCh + VIP strongly reduced Na⁺ but not Cl⁻ content in saliva, indicating
223 that VIP receptors are functionally expressed in SLG ducts. This finding revealed that Na⁺ and Cl⁻
224 reabsorption are independent processes in SLG. Such a non-coupled NaCl reabsorption mechanism
225 clearly differs from that observed in mouse SMG gland (5). Moreover, forskolin did not increase Na⁺
226 reabsorption, which clearly differs from the effect mediated by the cAMP-increasing agonists
227 isoproterenol (SMG) and VIP (SLG). The cAMP-mediated signals that originate from receptor-mediated
228 or adenylylate cyclase directly stimulated by forskolin might result in different responses from ion
229 transporting proteins involved in Na⁺ reabsorption.

230 In this study, we found that the K⁺ content in SMG saliva was higher than in SLG saliva. According to the
231 current salivary gland secretion model, the final K⁺ concentration of saliva is mostly determined by active
232 electro-diffusive K⁺ secretion via the K_{Ca1.1} (Kcnma1) channel (23). Consistent with this model, higher
233 levels of *Kcnma1* transcript levels were observed in mouse SMG compared to SLG tissue (13) supporting
234 our findings that the [K⁺] of saliva is higher in SMG (see Materials and Methods section for more details).

235 Given that Na⁺ reabsorption in SMG via ENaC is activated by an increase in intracellular cAMP levels
236 (5), we expected a higher K⁺ content in SMG saliva stimulated with CCh + isoproterenol due to the
237 depolarization caused by ENaC-mediated Na⁺ influx. However, co-stimulation with isoproterenol did not
238 increase the K⁺ content of SMG saliva. We do not have an explanation for this finding, but it is tempting
239 to speculate that K⁺ secretion might take place in a subset of duct cells that express K_{Ca1.1} but do not
240 express ENaC.

241 Little is known regarding K⁺ secretion by SLG, but it is assumed that K⁺ secretion occurs in duct cells.
242 Given that K⁺ content in saliva is inversely proportional to the flow rate, higher K⁺ content is expected

243 when SLG were co-stimulated with CCh + isoproterenol (which reduces flow rate). In contrast, K^+
244 content in SLG saliva was significantly reduced when SLG was stimulated with CCh + isoproterenol
245 compared to that obtained from SLG stimulated with only CCh. The same effect was also observed when
246 SLGs were stimulated with CCh + VIP. Furthermore, K^+ content in both SMG and SLG salivas was
247 significantly reduced when co-stimulated with forskolin. Our results differ from those reported by
248 Larsson et al. where they found that VIP and forskolin potentiated the CCh-mediated K^+ efflux in rat
249 parotid fragments (17). The differences between the studies could be due to 1) the different experimental
250 approaches (K^+ efflux measurements vs. K^+ content in saliva). In this case, a higher K^+ efflux caused by
251 the activation of a basolateral K^+ channel mediated by VIP and forskolin cannot be ruled out. 2) Different
252 species (rat vs. mouse) or gland (parotid vs. SMG-SLG).

253 Together, the data presented in this study show that VIP and IPR decrease K^+ secretion in the mouse
254 SLG. Additionally, the reduction in K^+ content in SMG and SLG in response to co-stimulation with
255 forskolin strongly suggests that a non-described, cAMP-dependent signaling pathway might directly
256 inhibit K^+ secretion in both glands.

257 Alternatively, given that K^+ and HCO_3^- secretion are coupled in salivary glands, we could assume a lower
258 HCO_3^- content in SLG saliva produced in response to CCh + IPR or CCh + VIP. Interestingly, there is
259 compelling evidence linking the structure of mucins with HCO_3^- ions, where lower HCO_3^- secretion is
260 associated with more viscous mucous in the airways (6). Together, a lower $KHCO_3$ secretion would result
261 in lower flow rates due to the higher viscosity of saliva.

262 Na^+ (and K^+ content) in SLG saliva was reduced when co-stimulated with CCh + VIP. Given that the Cl^-
263 was unaffected when co-stimulated with CCh + VIP and it is assumed that $[Na^+] + [K^+] = [Cl^-] + [HCO_3^-]$,
264 it is tempting to speculate that such co-stimulation might reduce the content of HCO_3^- in SLG saliva.
265 Further experiments are required to address this important topic.

266 Regarding calcium content, we found that the $[Ca^{2+}]$ of saliva was dramatically increased when β -
267 adrenergic receptors were co-stimulated with muscarinic receptors in SMG, but as expected, the β -
268 adrenergic receptor agonist IPR had no effect in SLG. Calcium concentration in SMG saliva increased by
269 140% when stimulated with carbachol + isoproterenol. On the other hand, SMG flow rate was decreased
270 by 12.4% when stimulated with carbachol + isoproterenol. Therefore, the increase in calcium content in
271 saliva collected in response to carbachol + isoproterenol cannot be explained by the lower flow rates
272 observed during carbachol + isoproterenol treatment.

273 Little is known regarding the mechanism underlying Ca^{2+} transport in salivary glands, but it has been
274 suggested that the final Ca^{2+} content in saliva is the result of two competing mechanisms, Ca^{2+} secretion
275 by acinar cells and Ca^{2+} reabsorption by duct cells (2). Based on our findings, the higher Ca^{2+} content
276 measured in SMG saliva stimulated with CCh+ IPR could be due to: 1) enhanced Ca^{2+} secretion by the
277 acinar epithelium; 2) decreased Ca^{2+} reabsorption by the duct epithelium; or, 3) activation of both Ca^{2+}
278 secretion and inhibition of Ca^{2+} reabsorption. Given that the Ca^{2+} content increased in SMG saliva when
279 glands were co-stimulated with CCh + isoproterenol, it was not surprising that a robust increase in Ca^{2+}
280 content was observed in SMG and SLG salivas when the glands were co-stimulated with CCh + forskolin.
281 Together, our results show that the mechanism(s) underlying Ca^{2+} transport by SMG and SLG strongly
282 depend on the intracellular levels of cAMP. However, VIP did not increase Ca^{2+} content in SMG and
283 SLG salivas, suggesting that other physiological secretagogues might be required to sufficiently raise
284 cAMP to affect Ca^{2+} transport by SMG and SLG.

285 The salivary mucins, which are mainly synthesized by the seromucous acinar cells of submandibular and
286 mucous cells of sublingual glands, form an adherent layer that coats the oral cavity where it plays a key
287 role in modulating the oral microbiome, hydration and lubrication of oral structures and teeth
288 remineralization and demineralization (31). In addition to the mucins, the oral mucus also consists of
289 other proteins and lipids secreted by mucous-secreting glands. Taking advantage of the *ex vivo* perfused
290 SMG/SLG preparation, which allows the evaluation of the direct effects of secretagogues on the SMG

291 and SLG function, we found that the activation of β -adrenergic receptors stimulates protein secretion by
292 SMG but not SLG (Figure 5). In contrast, vasoactive intestinal peptide (VIP) induced protein secretion in
293 both SMG and SLG. In summary, isoproterenol selectively activated protein secretion by SMG while VIP
294 induced protein secretion in both glands. Similar results to those displayed by VIP were obtained when
295 glands were co-stimulated with forskolin, which bypasses receptors to directly activate cAMP production.
296 Together, protein secretion by SMG and SLG are activated by increasing intracellular cAMP levels,
297 which suggest a similar molecular secretion mechanism in both glands albeit through different receptors.
298 Based on the activation profile of protein secretion by mouse salivary glands, the secretory acinar cells
299 responsible for the bulk of protein secretion express robust levels of β -adrenergic receptors in SMG. In
300 fact, detailed analysis of transcript levels revealed that the expression is higher for genes encoding β 1-
301 and β 2-adrenergic receptors (*Adrb1* and *Adrb2*) in SMG compared to SLG (See Material and Methods
302 Section) (13).

303 VIP induced protein secretion in both SMG and SLG saliva, suggesting that VIP receptors are expressed
304 in secretory cells from SMG and SLG. Considering that VIP also regulates duct function in SLG
305 (stimulates Na^+ reabsorption, see Figure 4E), transcript levels of *Vipr1* (which encodes for a type 1 VIP
306 receptor) were higher in SLG compared to SMG. On the other hand, transcript levels for type 2 VIP
307 receptors encoded by *Vipr2* were very low in both SLG and SMG (FPKM values <0.1) (See Material and
308 Methods Section).

309 In summary, in the current study we describe the development of a modification of the mouse SMG-
310 perfused preparation where both SMG and SLG are simultaneously perfused. Using this experimental
311 approach, we found that cAMP-mobilizing agents modulate diverse aspects of salivary gland function
312 such as flow rate, as well as the ion and protein compositions of saliva.

313

314

315 **Acknowledgments**

316 The authors want to thank Yasna Jaramillo for excellent technical assistance and Xin Gao for analyzing
317 and providing RNA-seq data.

318 **Grants**

319 This research was supported in part by the Intramural Research Program of the NIH, NIDCR 1-ZIA-
320 DE000738 (JEM) and 1-ZIG-DE000740 (NIDCR Veterinary Resources Core) and Proyecto Fondecyt
321 1171135 (MAC) of the Fondo Nacional de Ciencia y Tecnología (Chile).

322 **Disclosures**

323 The authors declare that they have no conflicts of interest with the contents of this article.

324 **Footnote**

325 The content is solely the responsibility of the authors and does not necessarily represent the official views
326 of the National Institutes of Health.

327

328 **References**

- 329 1. **Abe K, Yokota Y, and Dawes C.** Effects of parasympathomimetic and sympathomimetic drugs on
330 the secretion and composition of rat sublingual saliva. *J Dent Res* 61: 52-56, 1982.
- 331 2. **Bandyopadhyay BC, Swaim WD, Sarkar A, Liu X, and Ambudkar IS.** Extracellular Ca(2+) sensing
332 in salivary ductal cells. *J Biol Chem* 287: 30305-30316, 2012.
- 333 3. **Begenisich T, Nakamoto T, Ovitt CE, Nehrke K, Brugnara C, Alper SL, and Melvin JE.**
334 Physiological roles of the intermediate conductance, Ca2+-activated potassium channel Kcnn4. *J Biol*
335 *Chem* 279: 47681-47687, 2004.
- 336 4. **Catalan MA, Kondo Y, Pena-Munzenmayer G, Jaramillo Y, Liu F, Choi S, Crandall E, Borok Z,**
337 **Flodby P, Shull GE, and Melvin JE.** A fluid secretion pathway unmasked by acinar-specific Tmem16A
338 gene ablation in the adult mouse salivary gland. *Proc Natl Acad Sci U S A* 112: 2263-2268, 2015.
- 339 5. **Catalan MA, Nakamoto T, Gonzalez-Begne M, Camden JM, Wall SM, Clarke LL, and Melvin JE.**
340 Cfr and ENaC ion channels mediate NaCl absorption in the mouse submandibular gland. *J Physiol* 588:
341 713-724, 2010.
- 342 6. **Chen EY, Yang N, Quinton PM, and Chin WC.** A new role for bicarbonate in mucus formation.
343 *Am J Physiol Lung Cell Mol Physiol* 299: L542-549, 2010.
- 344 7. **Culp DJ, Graham LA, Latchney LR, and Hand AR.** Rat sublingual gland as a model to study
345 glandular mucous cell secretion. *Am J Physiol* 260: C1233-1244, 1991.
- 346 8. **Culp DJ, Zhang Z, and Evans RL.** Role of calcium and PKC in salivary mucous cell exocrine
347 secretion. *J Dent Res* 90: 1469-1476, 2011.
- 348 9. **Del Fiacco M, Quartu M, Ekstrom J, Melis T, Boi M, Isola M, Loy F, and Serra MP.** Effect of the
349 neuropeptides vasoactive intestinal peptide, peptide histidine methionine and substance P on human
350 major salivary gland secretion. *Oral Dis* 21: 216-223, 2015.
- 351 10. **Ekstrom J, and Ekman R.** Sympathectomy-induced increases in calcitonin gene-related peptide
352 (CGRP)-, substance P- and vasoactive intestinal peptide (VIP)-levels in parotid and submandibular glands
353 of the rat. *Arch Oral Biol* 50: 909-917, 2005.
- 354 11. **Ekstrom J, Mansson B, and Tobin G.** Vasoactive intestinal peptide evoked secretion of fluid and
355 protein from rat salivary glands and the development of supersensitivity. *Acta Physiol Scand* 119: 169-
356 175, 1983.
- 357 12. **Evans RL, Bell SM, Schultheis PJ, Shull GE, and Melvin JE.** Targeted disruption of the Nhe1 gene
358 prevents muscarinic agonist-induced up-regulation of Na(+)/H(+) exchange in mouse parotid acinar cells.
359 *J Biol Chem* 274: 29025-29030, 1999.
- 360 13. **Gao X, Oei MS, Ovitt CE, Sincan M, and Melvin JE.** Transcriptional profiling reveals gland-
361 specific differential expression in the three major salivary glands of the adult mouse. *Physiol Genomics*
362 50: 263-271, 2018.
- 363 14. **Ishikawa Y, Iida H, Skowronski MT, and Ishida H.** Activation of endogenous nitric oxide synthase
364 coupled with methacholine-induced exocytosis in rat parotid acinar cells. *J Pharmacol Exp Ther* 301: 355-
365 363, 2002.
- 366 15. **Kondo Y, Nakamoto T, Jaramillo Y, Choi S, Catalan MA, and Melvin JE.** Functional differences in
367 the acinar cells of the murine major salivary glands. *J Dent Res* 94: 715-721, 2015.
- 368 16. **Krane CM, Melvin JE, Nguyen HV, Richardson L, Towne JE, Doetschman T, and Menon AG.**
369 Salivary acinar cells from aquaporin 5-deficient mice have decreased membrane water permeability and
370 altered cell volume regulation. *J Biol Chem* 276: 23413-23420, 2001.
- 371 17. **Larsson O, Detsch T, and Fredholm BB.** VIP and forskolin enhance carbachol-induced K+ efflux
372 from rat salivary gland fragments by a Ca2(+)-sensitive mechanism. *Am J Physiol* 259: C904-910, 1990.

- 373 18. **Larsson O, and Olgart L.** The enhancement of carbachol-induced salivary secretion by VIP and
374 CGRP in rat parotid gland is mimicked by forskolin. *Acta Physiol Scand* 137: 231-236, 1989.
- 375 19. **Ma T, Song Y, Gillespie A, Carlson EJ, Epstein CJ, and Verkman AS.** Defective secretion of saliva
376 in transgenic mice lacking aquaporin-5 water channels. *J Biol Chem* 274: 20071-20074, 1999.
- 377 20. **Martinez JR.** Ion transport and water movement. *J Dent Res* 66 Spec No: 638-647, 1987.
- 378 21. **Martinez JR, and Cassity N.** Effect of transport inhibitors on secretion by perfused rat
379 submandibular gland. *Am J Physiol* 245: G711-716, 1983.
- 380 22. **Melvin JE, Yule D, Shuttleworth T, and Begenisich T.** Regulation of fluid and electrolyte
381 secretion in salivary gland acinar cells. *Annu Rev Physiol* 67: 445-469, 2005.
- 382 23. **Nakamoto T, Romanenko VG, Takahashi A, Begenisich T, and Melvin JE.** Apical maxi-K (KCa1.1)
383 channels mediate K⁺ secretion by the mouse submandibular exocrine gland. *Am J Physiol Cell Physiol*
384 294: C810-819, 2008.
- 385 24. **Nakamoto T, Srivastava A, Romanenko VG, Ovitt CE, Perez-Cornejo P, Arreola J, Begenisich T,**
386 **and Melvin JE.** Functional and molecular characterization of the fluid secretion mechanism in human
387 parotid acinar cells. *Am J Physiol Regul Integr Comp Physiol* 292: R2380-2390, 2007.
- 388 25. **Nauntofte B.** Regulation of electrolyte and fluid secretion in salivary acinar cells. *Am J Physiol*
389 263: G823-837, 1992.
- 390 26. **Proctor GB.** The physiology of salivary secretion. *Periodontol* 2000 70: 11-25, 2016.
- 391 27. **Proctor GB, and Carpenter GH.** Regulation of salivary gland function by autonomic nerves.
392 *Auton Neurosci* 133: 3-18, 2007.
- 393 28. **Romanenko V, Nakamoto T, Srivastava A, Melvin JE, and Begenisich T.** Molecular identification
394 and physiological roles of parotid acinar cell maxi-K channels. *J Biol Chem* 281: 27964-27972, 2006.
- 395 29. **Romanenko VG, Catalan MA, Brown DA, Putzier I, Hartzell HC, Marmorstein AD, Gonzalez-**
396 **Begne M, Rock JR, Harfe BD, and Melvin JE.** Tmem16A encodes the Ca²⁺-activated Cl⁻ channel in mouse
397 submandibular salivary gland acinar cells. *J Biol Chem* 285: 12990-13001, 2010.
- 398 30. **Romanenko VG, Nakamoto T, Srivastava A, Begenisich T, and Melvin JE.** Regulation of
399 membrane potential and fluid secretion by Ca²⁺-activated K⁺ channels in mouse submandibular glands. *J*
400 *Physiol* 581: 801-817, 2007.
- 401 31. **Tabak LA.** In defense of the oral cavity: structure, biosynthesis, and function of salivary mucins.
402 *Annu Rev Physiol* 57: 547-564, 1995.
- 403 32. **Yang YD, Cho H, Koo JY, Tak MH, Cho Y, Shim WS, Park SP, Lee J, Lee B, Kim BM, Raouf R, Shin**
404 **YK, and Oh U.** TMEM16A confers receptor-activated calcium-dependent chloride conductance. *Nature*
405 455: 1210-1215, 2008.

406

407 **Figure Legends.**

408 **Figure 1. Simultaneous perfusion of mouse submandibular and sublingual glands.** Image depicting
409 SMG and SLG perfused via common carotid artery by a 31G cannula. SMG and SLG main ducts were
410 separated and connected to different calibrated glass capillary tubes for collecting saliva to quantify flow
411 rates and performing ion and protein analysis.

412 **Figure 2. *Ex vivo* flow rates and ion composition of SMG and SLG saliva upon combined**
413 **muscarinic acetylcholine and β -adrenergic receptor activation.** **A.** Flow rates for SMGs (10 minutes
414 of stimulation) perfused with 0.3 μ M CCh (black circles, n=14 glands) or 0.3 μ M CCh + 5 μ M IPR (grey
415 circles, n=13 glands) bicarbonate-containing solutions. **B.** Total amount of saliva secreted by SMGs
416 stimulated with 0.3 μ M CCh (black diamonds) or 0.3 μ M CCh + 5 μ M IPR (grey diamonds). Boxes
417 correspond to the average (line) \pm standard deviation (SD) of experiments shown in panel **A**. **C-D.** Na^+ ,
418 K^+ and Cl^- (**C**) and Ca^{2+} (**D**) concentrations (mM) in SMG saliva stimulated with 0.3 μ M CCh (black
419 diamonds, n=14 except for Ca^{2+} measurements where the n=8) or 0.3 μ M CCh + 5 μ M IPR (grey
420 diamonds, n=13 except for Ca^{2+} measurements where the n=8). **E.** Flow rates for SLGs (10 minutes of
421 stimulation) perfused with 0.3 μ M CCh (black circles, n=14 glands) or 0.3 μ M CCh + 5 μ M IPR (grey
422 circles, n=14 glands) bicarbonate-containing solutions. **F.** Total amount of saliva secreted by SMGs
423 stimulated with 0.3 μ M CCh (black diamonds) or 0.3 μ M CCh + 5 μ M IPR (grey diamonds). Boxes
424 correspond to the average (line) \pm SD of experiments shown in panel **E**. **G-H.** Na^+ , K^+ and Cl^- (**G**) and
425 Ca^{2+} (**H**) concentrations (mM) in SLG saliva stimulated with 0.3 μ M CCh (black diamonds, n=14 except
426 for Ca^{2+} measurements where the n=5) or 0.3 μ M CCh + 5 μ M IPR (grey diamonds, n=14 except for Ca^{2+}
427 measurements where the n=4). * and ** $p < 0.05$ and < 0.01 , respectively (Student's t test). Box graphs
428 correspond to the average (line) \pm SD for each experimental condition.

429 **Figure 3. Effect of cAMP-raising secretagogues on the *ex vivo* secretions by SMG and SLG.** **A.** Flow
430 rates for SMGs (15 minutes of stimulation) stimulated with 0.3 μ M CCh (white circles, n=8 glands) or 0.3

431 μM CCh + 10 μM forskolin (grey circles, n=11 glands) or + 100 nM VIP (black circles, n=6 glands). **B.**
432 Total amount of saliva secreted by SMGs stimulated with the secretagogues shown in panel **A**. **C.** Flow
433 rates for SLGs (15 minutes of stimulation) stimulated with 0.3 μM CCh (white circles, n=11) or 0.3 μM
434 CCh + 10 μM forskolin (grey circles, n=15) or + 100 nM VIP (black circles, n=11). **D.** Total amount of
435 saliva secreted by SMGs stimulated with the secretagogues shown in **C**. Box graphs correspond to the
436 average (line) \pm SD for each experimental condition. * $p < 0.05$ (ANOVA followed by Bonferroni's *post*
437 *hoc* test).

438 **Figure 4. Effect of cAMP-raising secretagogues on the ion composition of SMG and SLG salivas.**
439 Na^+ (**A**), Cl^- (**B**), K^+ (**C**) and Ca^{2+} (**D**) concentrations of SMG saliva (from Figure 3) stimulated with 0.3
440 μM CCh (white circles, n=14) or 0.3 μM CCh + 10 μM forskolin (grey circles, n=10) or + 100 nM VIP
441 (black circles, n=6). Na^+ (**E**), Cl^- (**F**), K^+ (**G**) and Ca^{2+} (**H**) concentrations of SLG saliva (from Figure 3)
442 stimulated with 0.3 μM CCh (white circles; Na^+ : n=6, Cl^- : n=6, K^+ : n=6, Ca^{2+} : n=5) or 0.3 μM CCh + 10
443 μM forskolin (grey circles; Na^+ : n=8, Cl^- : n=9, K^+ : n=8, Ca^{2+} : n=4) or + 100 nM VIP (black circles; Na^+ :
444 n=7, Cl^- : n=7, K^+ : n=7, Ca^{2+} : n=4). Box graphs correspond to the average (line) \pm SD for each
445 experimental condition. * $p < 0.05$ (ANOVA followed by Bonferroni's *post hoc* test).

446 **Figure 5. Effect of β -adrenergic agonist on the protein secretion by SMG and SLG.** **A-C.** Protein
447 concentration (**A**), amount of saliva secreted (**B**) and total amount of protein secreted (**C**) by SMG (5
448 minutes of stimulation) in response to 0.3 μM CCh (black circles, n=9) or 0.3 μM CCh + 5 μM IPR (grey
449 circles, n=6). **D-F.** Protein concentration (**D**), amount of saliva secreted (**E**) and total amount of protein
450 secreted (**F**) by SLG (5 minutes of stimulation) in response to 0.3 μM CCh (black circles, n=9) or 0.3 μM
451 CCh + 5 μM IPR (grey circles, n=7). Total amount of protein was calculated by multiplying the protein
452 concentration by the secreted saliva volume. Box graphs correspond to the average (line) \pm SD of
453 experiments. ** $p < 0.01$ (Student's *t* test).

454 **Figure 6. Effect of cAMP-raising secretagogues on the protein secretion by SMG and SLG. A-C.**
455 Protein concentration (**A**), amount of saliva secreted (**B**) and total amount of protein secreted (**C**) by SMG
456 (5 minutes of stimulation) in response to 0.3 μ M CCh (white circles, n=9) or 0.3 μ M CCh + 10 μ M
457 forskolin (grey circles, n=12) or + 100 nM VIP (black circles, n=8). **D-F.** Protein concentration (**D**),
458 amount of saliva secreted (**E**) and total amount of protein secreted (**F**) by SLG (5 minutes of stimulation)
459 in response to 0.3 μ M CCh (white circles, n=9) or 0.3 μ M CCh + 10 μ M forskolin (grey circles, n=10) or
460 + 100 nM VIP (black circles, n=7). Box graphs correspond to the average (line) \pm SD of experiments. *
461 $p < 0.05$ (ANOVA followed by Bonferroni's *post hoc* test).

Figure 1

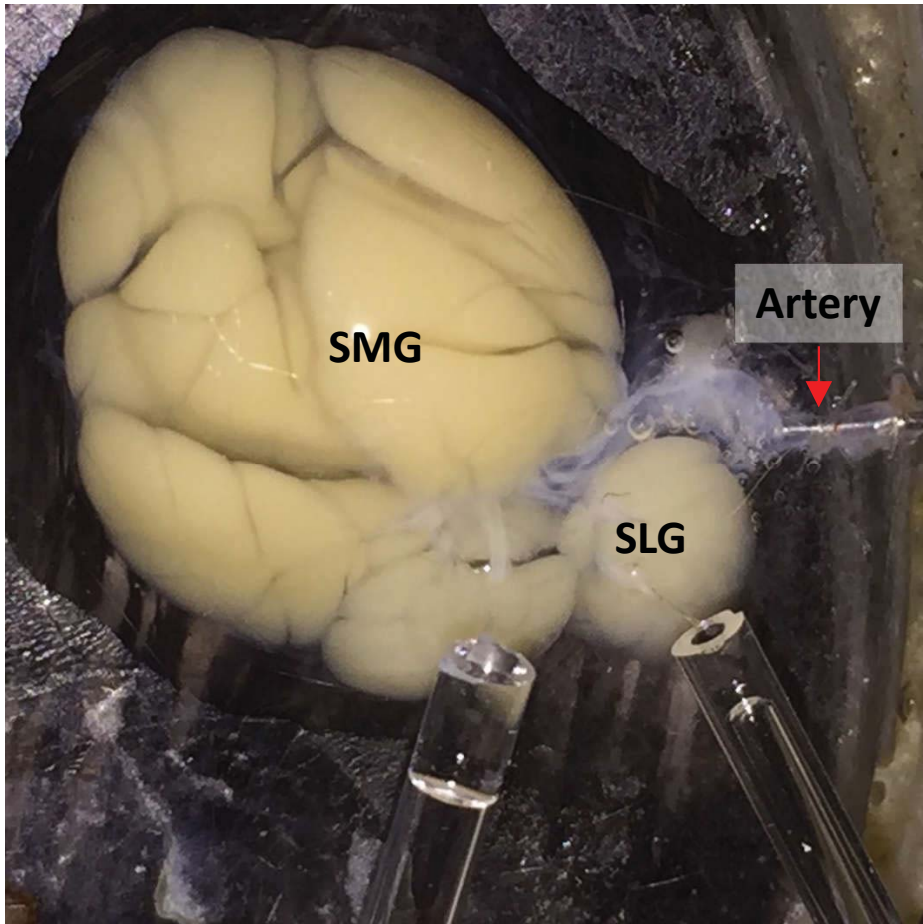
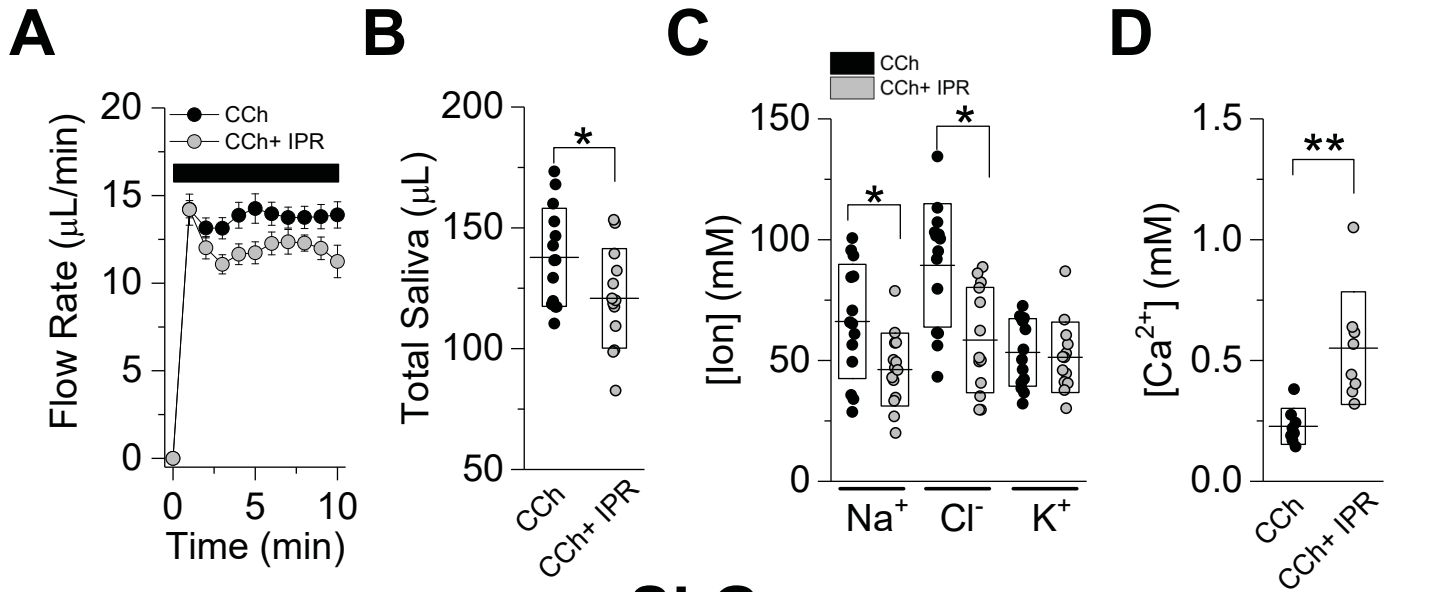


Figure 2

SMG



SLG

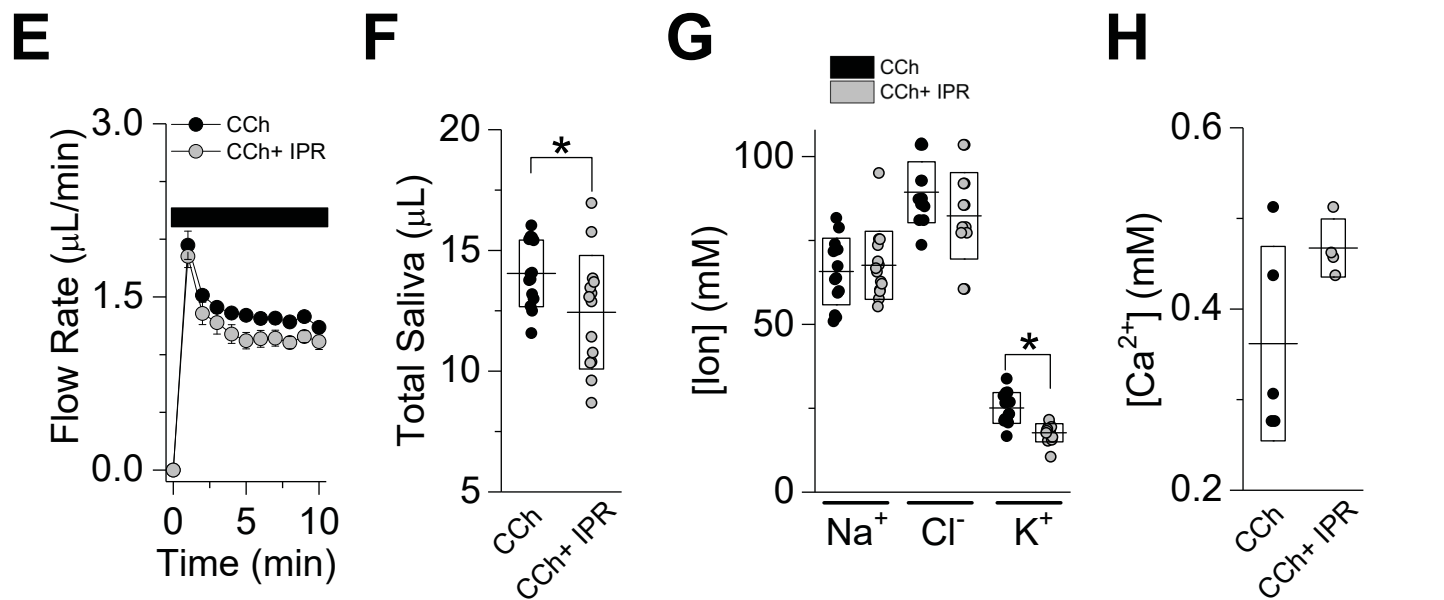
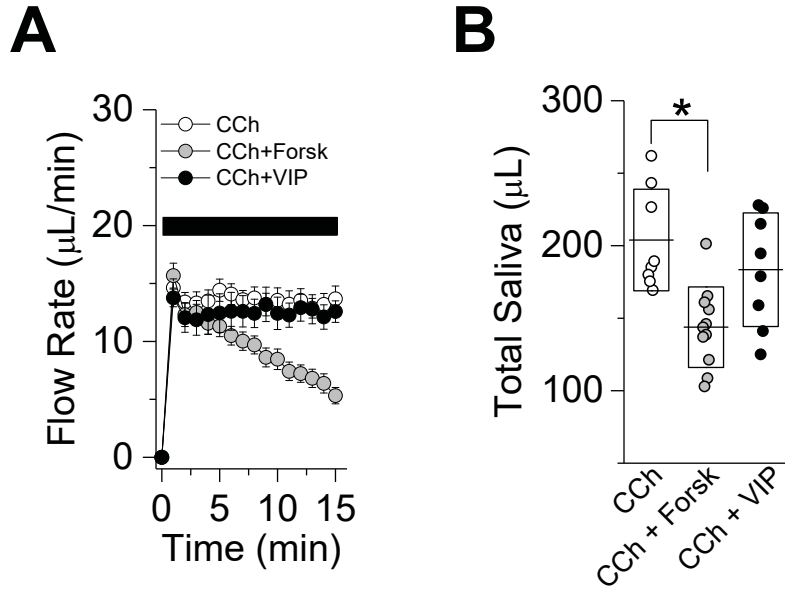


Figure 3

SMG



SLG

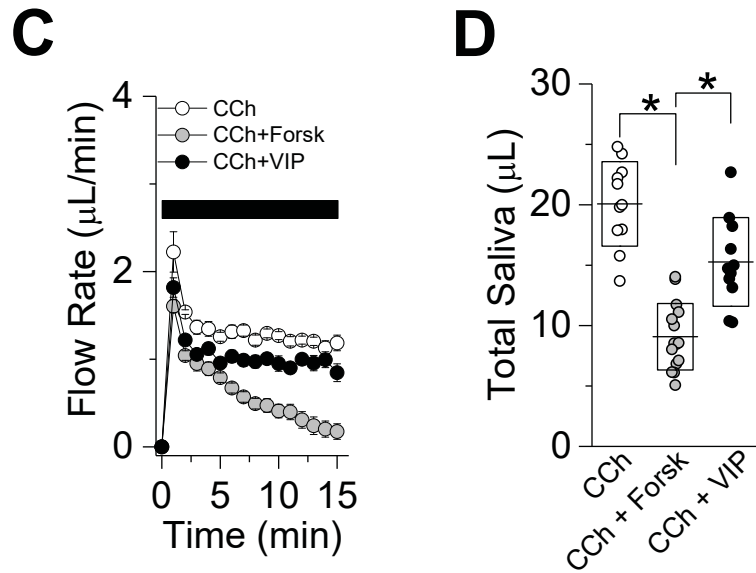
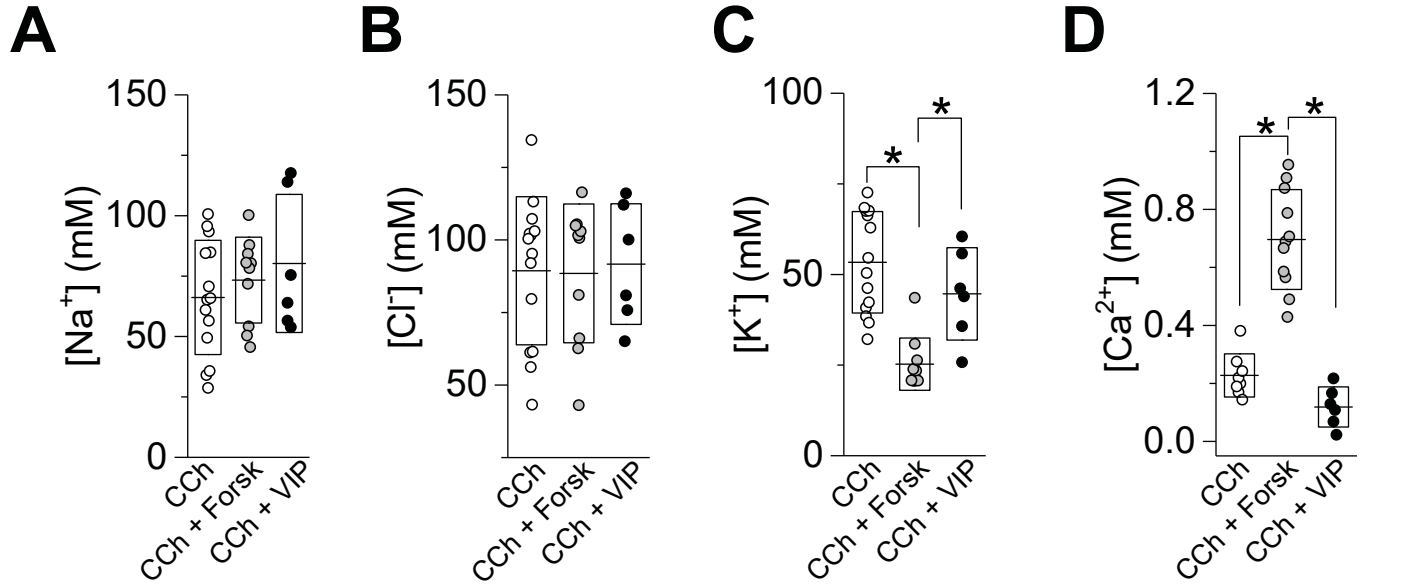


Figure 4

SMG



SLG

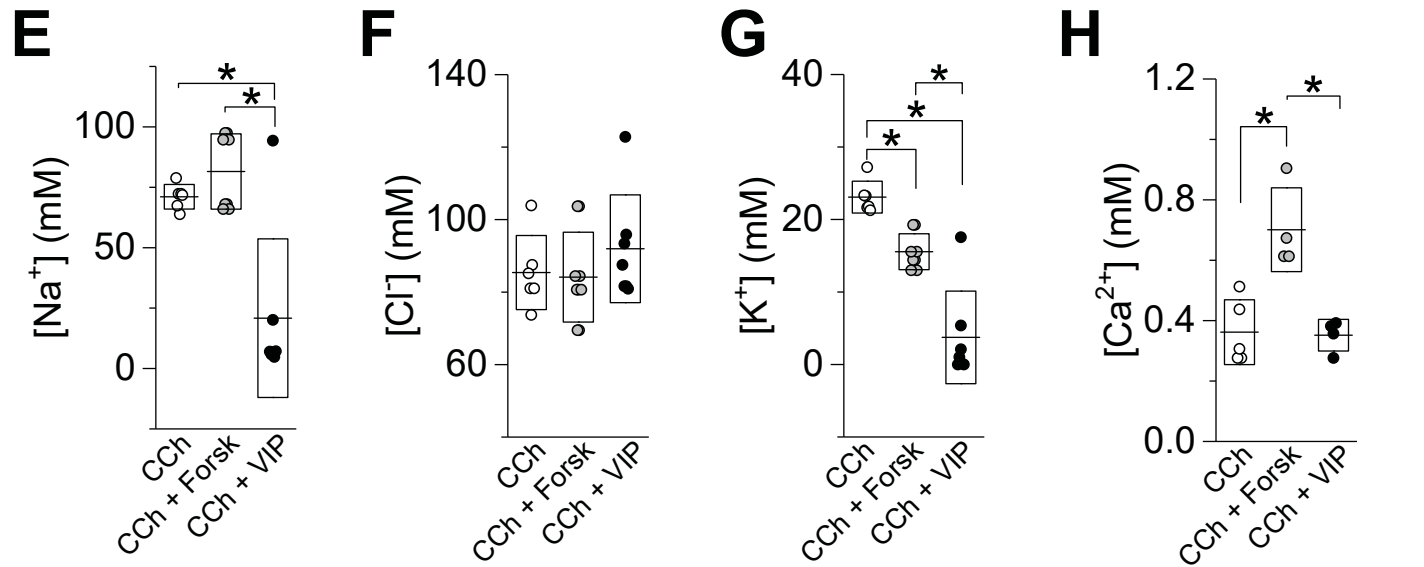
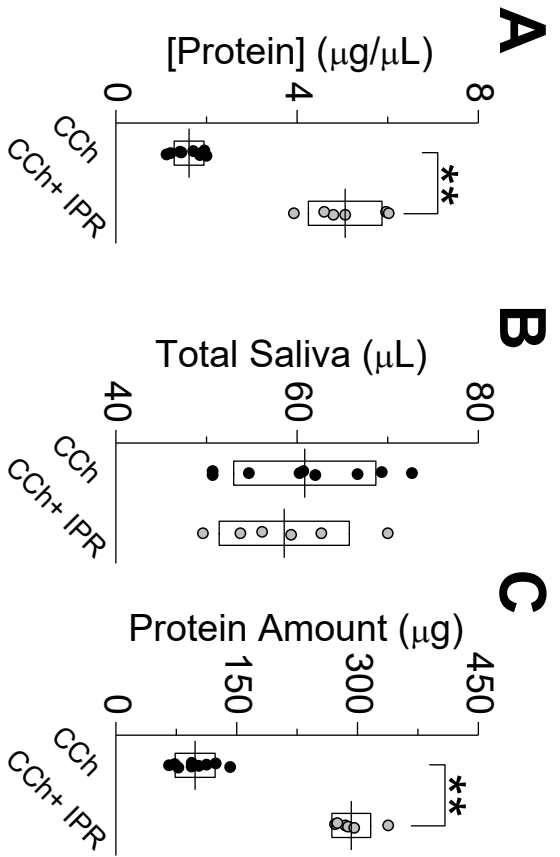


Figure 5

SMG



SLG

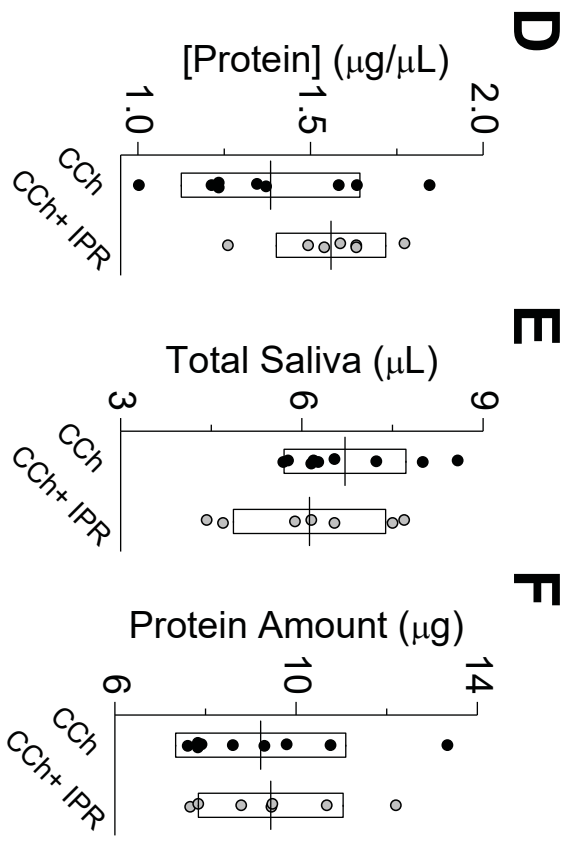
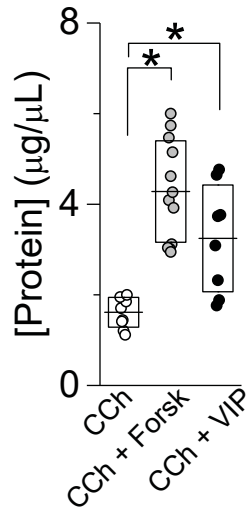


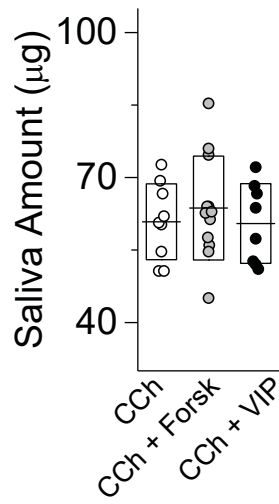
Figure 6

SMG

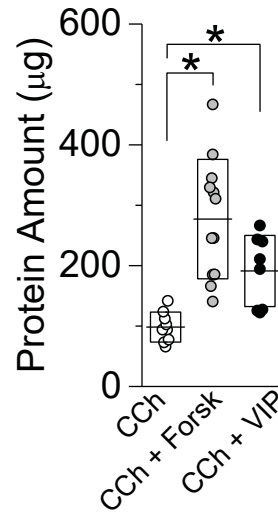
A



B

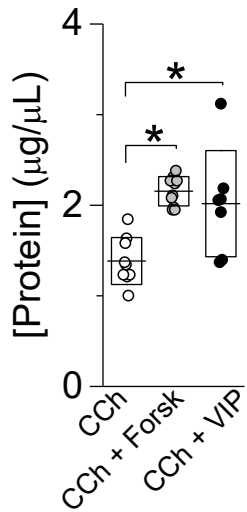


C

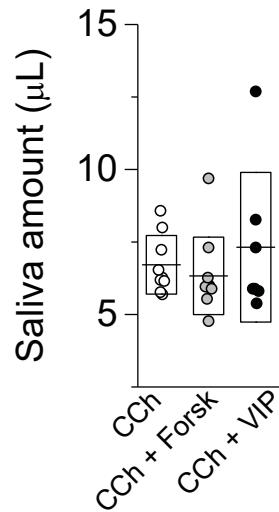


SLG

D



E



F

